Polymers for Tissue Engineering

Editors:
M.S. Shoichet and J.A. Hubbell

VSP
Utrecht, The Netherlands, 1998

VSP BV
P.O. Box 346
3700 AH Zeist
The Netherlands

Tel: +31 30 692 5790
Fax: +31 30 693 2081
E-mail: vsppub@compuserve.com
Home Page: http://www.vsppub.com

First published in 1998

ISBN 90-6764-289-4

Printed in The Netherlands by Ridderprint bv, Ridderkerk.

Polymers for Tissue Engineering, pp. 221–234
Molly S. Shoichet and Jeffrey A. Hubbell (Eds)

Surface characteristics and biocompatibility of lactide-based poly(ethylene glycol) scaffolds for tissue engineering

DONG KEUN HAN [1], KI DONG PARK [1], JEFFREY A. HUBBELL [2] and YOUNG HA KIM [1,*]

[1] *Biomaterials Research Center, Korea Institute of Science and Technology, P.O. Box 131, Cheongryang, Seoul 130-650, Korea*
[2] *Department of Materials and Institute for Biomedical Engineering, ETH Zürich and University of Zürich, CH-8044 Zürich, Switzerland*

Received 25 August 1997; accepted 17 December 1997

Abstract—Novel lactide-based poly(ethylene glycol) (PEG) polymer networks (GL9-PEGs) were prepared by UV copolymerization of a glycerol-lactide triacrylate (GL9-Ac) with PEG monoacrylate (PEG-Ac) to use as scaffolds in tissue engineering, and the surface properties and biocompatibility of these networks were investigated as a function of PEG molecular weight and content. Analysis by ATR-FTIR and ESCA reveled that PEG was incorporated well within the GL9-PEG polymer networks and was enriched at the surfaces. From the results of SEM, AFM, and contact angle analyses, GL9-PEG networks showed relatively rough and irregular surfaces compared to GL9 network, but the mobile PEG chains coupled at their termini were readily exposed toward the aqueous environment when contacting water such that the surfaces became smoother and more hydrophilic. This reorientation and increase in hydrophilicity were more extensive with increasing PEG molecular weight and content. As compared to GL9 network lacking PEG, protein adsorption as well as platelet and *S. epidermidis* adhesion to GL9-PEG networks were significantly reduced as the molecular weight and content of PEG was increased, indicating that GL9-PEG networks are more biocompatible than the GL9 network due to PEG's passivity. Based on the physical and biological characterization reported, the GL9-PEG materials would appear to be interesting candidates as matrices for tissue engineering.

Key words: Tissue engineering; scaffold; polylactide; PEG; hydrophilicity; biocompatibility.

INTRODUCTION

Biomaterials play an important role in tissue engineering [1, 2]. Polymeric biomaterials in tissue engineering research are being applied in conducting, guiding,

*To whom correspondence should be addressed. E-mail: yhakim@kistmail.kist.re.kr

and inducing tissue formation as well as in blocking tissue interactions [3, 4]. These polymers for structural scaffolds require proper physical and mechanical properties, designable biodegradability, nontoxicity, good biocompatibility, and the ability to interact with specific cells. Scaffolds meeting these requirements may be useful regenerating damaged tissues or organs by combining scaffolds with living cells.

From the perspective of scaffold biocompatibility, one would like to be able to limit protein adsorption and cellular interactions with the scaffold's base material, thus permitting specific cell adhesion to be designed separately via the incorporation of cell adhesion peptides [4]. Moreover, it is desirable that interactions with potentially colonizing bacteria be minimized. A variety of approaches have been taken to accomplish these ends in improving the biocompatibility of polymer surfaces [5, 6]. Surface modification, for example, has been explored by: (1) chemical grafting of a hydrophilic component, such as poly(ethylene glycol) (PEG); (2) incorporating bioactive agents such as anticoagulant (heparin), platelet-passivating prostaglandins (e.g. PGE_1), and fibrinolytic enzymes (tPA); and (3) biological modification using protein adsorption or cell seeding.

PEG is a hydrophilic synthetic polymer and has received much attention because it is highly water soluble compared with other similar polyethers. PEG's passivity to biological responses may be caused by many factors, such as a very low interfacial free energy with water, lack of ionic binding sites, high chain mobility, steric stabilization effects, and molecular conformation in water [7]. These characteristics have led to many investigations on the utilization of PEG as a biocompatible material. It has been reported that PEG-treated biomaterials showed less protein adsorption [8], platelet and cell adhesion [9, 10], and bacteria adhesion [11] due to the characteristics listed above. The antigenicity and immune clearance of therapeutic proteins have also been shown to be reduced by grafting of PEG [12]. PEG has almost been introduced into polymer substrates by physical adsorption [13] and entrapment [14], covalent coupling [15, 16], photoinduced grafting [17], glow discharge treatment [18], and gamma irradiation [7] to improve their biocompatibility. Covalent coupling of PEG to substrates is usually the most effective way to provide stable performance for biomedical applications.

Recently, we have developed novel polymer network scaffolds for use in tissue engineering, which have biodegradable, biocompatible, and ligand-immobilizable characteristics [19, 20]. Lactide-based PEG-containing scaffolds were synthesized by UV copolymerization using two nontoxic precusors, triacrylated lactic acid oligomer emanating from a glycerol center and monoacrylated PEG (PEG-Ac). The obtained cross-linked polymer networks were glassy and transparent. All such networks showed low swelling in water and had no melting endotherms, but displayed a glass transition temperature that was indicative of phase-mixing of the PEG. The mobile PEG chains in the copolymer networks were enriched at the surfaces and made the surfaces more hydrophilic. In addition, PEG-containing networks were highly resistant to fibroblasts adhesion compared to glass as well as network lacking PEG.

In this study we have focused our attention on one particularly favorable triacrylated lactide oligomer macromonomer emanating from a glycerol center, with lactide arms of average degree of polymerization 9 (thus, GL9-Ac). We have performed a detailed analysis of surface character and investigated interactions with proteins, platelets, and bacteria as PEG molecular weight and content were varied.

MATERIALS AND METHODS

Synthesis of GL9-PEG networks

Figure 1 shows the synthetic reactions leading to the formation of GL9-PEG networks. The synthetic methods employed to obtain GL triols, GL triacrylates, and GL-PEG networks have been previously reported in detail elsewhere [19, 20]. Networks were formed from two reactive precursors, a GL9-Ac and α-monoacrylate-ω-monohydroxy PEG (PEG-Ac; M_w = 1000, 1K; 4000, 4K; 8000, 8K; Monomer-Polymer & Dajac).

The typical synthetic procedure is as follows: first, 1.02 g glycerol (G, Aldrich), 43.2 g L-lactide (L, 27 mol per G mol; Aldrich), and 0.61 g stannous octoate (St-Oct, 1/200 of L mol; Sigma) were reacted in melt at 130°C for 6 h under argon. The melt was allowed to cool and was dissolved in chloroform, micro-filtered, precipitated in hexane, and vacuum-dried to yield GL9 triol. Second, 4.77 g acryloyl chloride (AcCl, 6 mol per GL9 triol mol; Aldrich) dissolved in 18 ml of dichloromethane (DCM) was slowly dropped into 35 g GL9 triol and 5.33 g triethylamine (TEA, 1 mol per AcCl mol; Aldrich) dissolved in 315 ml of DCM and reacted at 0°C for 6 h and at room temperature for 42 h. The solution was micro-filtered, precipitated in diethylether, and vacuum-dried to yield triacrylated GL9, GL9-Ac. Finally, a 25% w/v solution of 1 g GL9-Ac, PEG-Ac (10, 20, and 30 wt% of GL9-Ac), and 1% w/w 2,2-dimethoxy-2-phenylacetophenone (benzyl dimethyl ketal, BDMK; Aldrich) dissolved in DCM were copolymerized by a 100-W medium pressure mercury ultraviolet (UV) irradiation (Black-Ray Model B-100A, 365 nm, UV Products) on Petri dishes to obtain GL9-PEG networks. The photocopolymerization was continued until gelation occurred, typically 10 min. The GL9-PEG network films produced were dried under vacuum at 60°C for 1 day, and then extracted with chloroform at room temperature for 1 day to remove unreacted macromers and homopolymers. The films were dried again and used for surface characterization and biocompatibility analysis.

The synthesized networks were denoted as follows: GL9-PEGnK-p, where 9 is the total number of dimeric repeats of lactic acid, n (1, 4, and 8) is the molecular weight (K = 1000) of PEG-Ac, and p (10, 20, and 30) is weight % of PEG-Ac per GL9-Ac. In addition, GL9 homonetwork was prepared using only GL9-Ac in the absence of PEG-Ac for comparison.

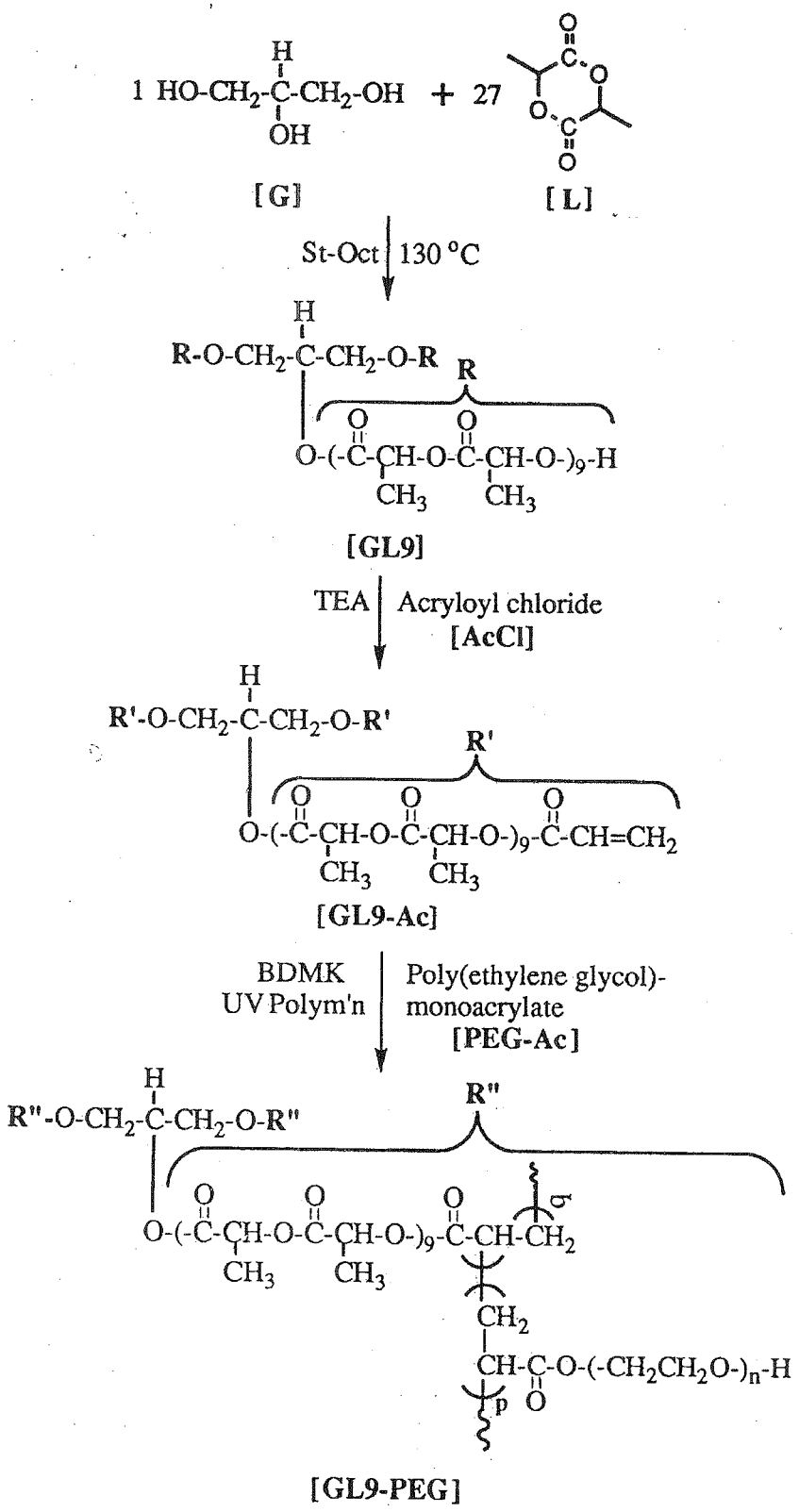

Figure 1. Scheme for synthesis of GL9-PEG networks.

Surface characterization

Attenuated total reflectance–Fourier transform infrared (ATR-FTIR) spectra were obtained from the surfaces of the networks using a Mattson Genesis Series FTIR spectrophotometer. The elemental compositions of the surfaces were determined using an electron spectroscopy for chemical analysis (ESCA) spectrometer (S-Probe Surface Science) at a take-off angle of 55 deg. The subpeaks of C_{1s} were deconvoluted using a curve-fitting method from a series of Gaussian–Lorentzian curves [21].

The surface morphology of networks was examined with a Hitachi S-2460N scanning electron microscopy (SEM) at an accelerating voltage of 19 kV. Samples were mounted and then sputter-coated with gold using an ion coater (Hitachi E-1010). Atomic force microscopy (AFM) in contact mode (DC mode) was performed with an Autoprobe CP system from Park Scientific Instruments (PSI, Sunnyvale, CA, USA). Images were obtained from dry and wet (hydrated in water for 1 day) sample surfaces in air using a 100-μm piezo-scanner and a microfabricated triangular cantilever supporting an integrated pyramidal tip (Ultralever™, PSI).

Surface wettability was assessed by two methods: static contact angles [22] were measured by the sessile drop method using an Erma Contact Anglemeter G-I, and dynamic contact angles (DCA) [23] were determined by the Wilhelmy plate method using a DCA-315 apparatus (Cahn Instruments) in water.

Biocompatibility

Measurements of protein adsorption were carried out by ESCA. Human plasma (Sigma) was diluted with phosphate-buffered saline (PBS, pH 7.4) to make a 10% solution. The polymer network samples (1×1 cm^2) were placed on 12-well polystyrene plates (Corning) and equilibrated with PBS for 1 h. After removing the PBS solution from the wells by pipetting, the plasma protein solution (4 ml) was added to the wells. After 1 h incubation at 37°C, the samples were washed with PBS, followed by washing with water to remove nonadsorbed proteins. After vacuum drying, the protein-adsorbed sample surfaces were analyzed by ESCA [24]. The N_{1s} peaks from the detailed scan spectra were used as a measure of the amount of proteins adsorbed on the surfaces.

Measurements of platelet adhesion were carried out with human platelet-rich plasma (PRP). Whole blood, anticoagulated with citrate, was centrifuged at 300 *g* for 10 min to obtain PRP. The platelet concentration of PRP was adjusted to 2×10^4 platelets μl^{-1} by adding platelet-por plasma to PRP. Sample films (1×1 cm^2) prehydrated for 24 h in PBS were immersed in the diluted PRP. After 2 h incubation at 37°C, unadhered platelets in the PRP were counted by a hematocytometer. The amount of platelets that adhered upon the film was calculated by subtracting the number of unadhered platelets from the number of diluted platelets that were initially incubated.

S. epidermidis (ATCC no. 12228), a Gram-positive bacterial strain, was used for measurement of bacterial adhesion to the networks. The films (1×1 cm^2) were incubated in human plasma, which had been diluted to 80% with tryptic soy broth (TSB, DIFCO), inoculated with 2×10^6 bacteria ml^{-1} for 24 h at 37°C with constant swirling. After the films were washed with PBS, the bacteria were eluted from the surface using an ultrasonicator. The bacteria eluted in PBS were diluted, incubated on agar plates for 19 h at 37°C, and then counted as single colony-forming unit (CFU).

RESULTS AND DISCUSSION

Synthesis and surface properties

The structure of reaction intermediates, GL9 triol and GL9 triacrylate, was confirmed by elemental analysis, FTIR, and NMR. The obtained GL9 network films were glassy and transparent and the gel content of the networks that were formed by crosslinking was typically 90%. The bulk and some surface characteristics as well as fibroblasts adhesion of these polymer networks have been described in detail elsewhere [20].

Figure 2 shows typical ATR-FTIR spectra of GL9 and GL9-PEG8K-20 surfaces. While three sharp peaks at 1082, 1182, and 1750 cm^{-1} were attributed to C—O, antisymmetric C—O, and C=O stretchings from GL9 network, a strong broad band of C—O stretching in PEG was observed at 1000–1150 cm^{-1} for the GL9-PEG8K-20 network. Although the C—O peaks from lactide in GL9 and from PEG in GL9-PEG networks were overlapped, the composite C—O peak was broader with increasing molecular weight and content of PEG.

Table 1 shows the atomic surface composition of GL9 and GL9-PEG networks analyzed by ESCA. After the incorporation of PEG in the GL9 network, the oxygen atomic percentage of the GL9-PEG networks considerably increased at the expense of a decrease in the carbon atomic percentage. From the results of analysis of the C_{1s} peaks obtained from curve fitting, no PEG ether peak was founded in the

Table 1.
ESCA results for GL9 and GL9-PEG networks

Material	C	O	C—O/C—C[a]
GL9 network	72	28	0
GL9-PEG1K-20	64	36	0.11
GL9-PEG4K-10	64	36	0.16
GL9-PEG4K-20	65	35	0.18
GL9-PEG4K-30	67	33	0.19
GL9-PEG8K-20	67	33	0.21

[a] Ratio of PEG ether (C—O) % (286.5 eV) over GL hydrocarbon (C—C) % (285.0 eV) from C_{1s} high resolution spectra.

GL9 network. As the PEG molecular weight and content in GL9-PEG networks were increased, the oxygen atomic percentage was relatively decreased, but the value of PEG ether percentage over the GL hydrocarbon percentage increased, suggesting that PEG was enriched at the network surfaces. This enrichment was observed both as PEG-Ac molecular weight was increased at constant PEG mass content and as PEG content was increased at constant PEG molecular weight.

The surface morphology of GL9 networks was examined by SEM and AFM. Figure 3 shows typical SEM micrographs of GL9 and GL9-PEG8K-20 surfaces. The GL9 surface was relatively smooth, whereas GL9-PEG surfaces were more rough and irregular, irrespective of the molecular weight and content of PEG incorporated. To study further the irregularities and reorientation of GL9-PEG surfaces in the dried and hydrated states, AFM observation was carried out, as shown in Figs 4 and 5. The GL9 surface in the dry state was considerably smooth and homogeneous, but GL9 in the wet state became relatively rough. In addition, the GL9-PEG surface in the dry state was very rough and heterogeneous, perhaps due to partial coverage by PEG chains on the surface. After hydration in water for 1 day, the GL9-PEG surface became more smooth. This surface roughness of dry GL9-PEG networks increased gradually with increments in PEG molecular weight and content. It was proved from statistical analysis of the roughness measurement that rms roughness of the wetted GL9 surface (47 Å) was increased compared to that of the dried one (28 Å). On the contrary, the wetted GL9-PEG surface (420 Å) showed much less rms roughness than did the dried one (700 Å), suggesting that the flexible PEG chains coupled within the GL9-PEG network were reoriented into the aqueous environment and more completely covered on the surface. Such a phenomenon was also supported from 3D images of network surfaces (Fig. 5). As

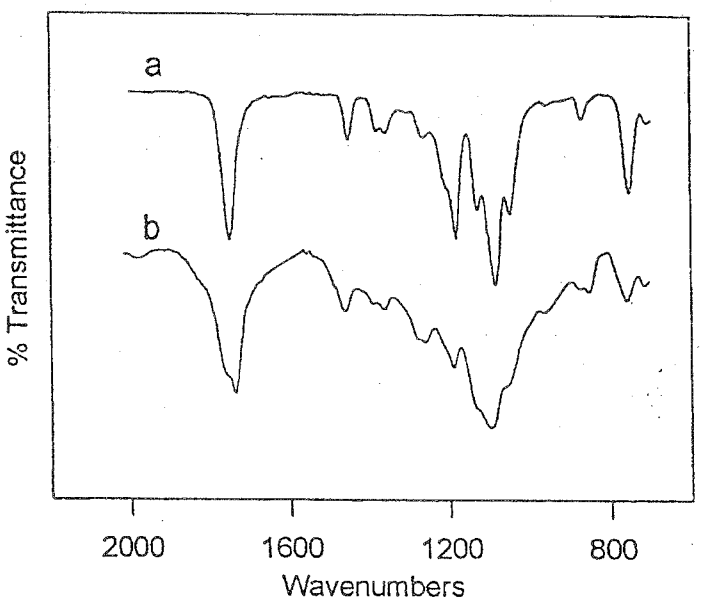

Figure 2. Typical ATR-FTIR spectra of (a) GL9 and (b) GL9-PEG8K-20 surfaces.

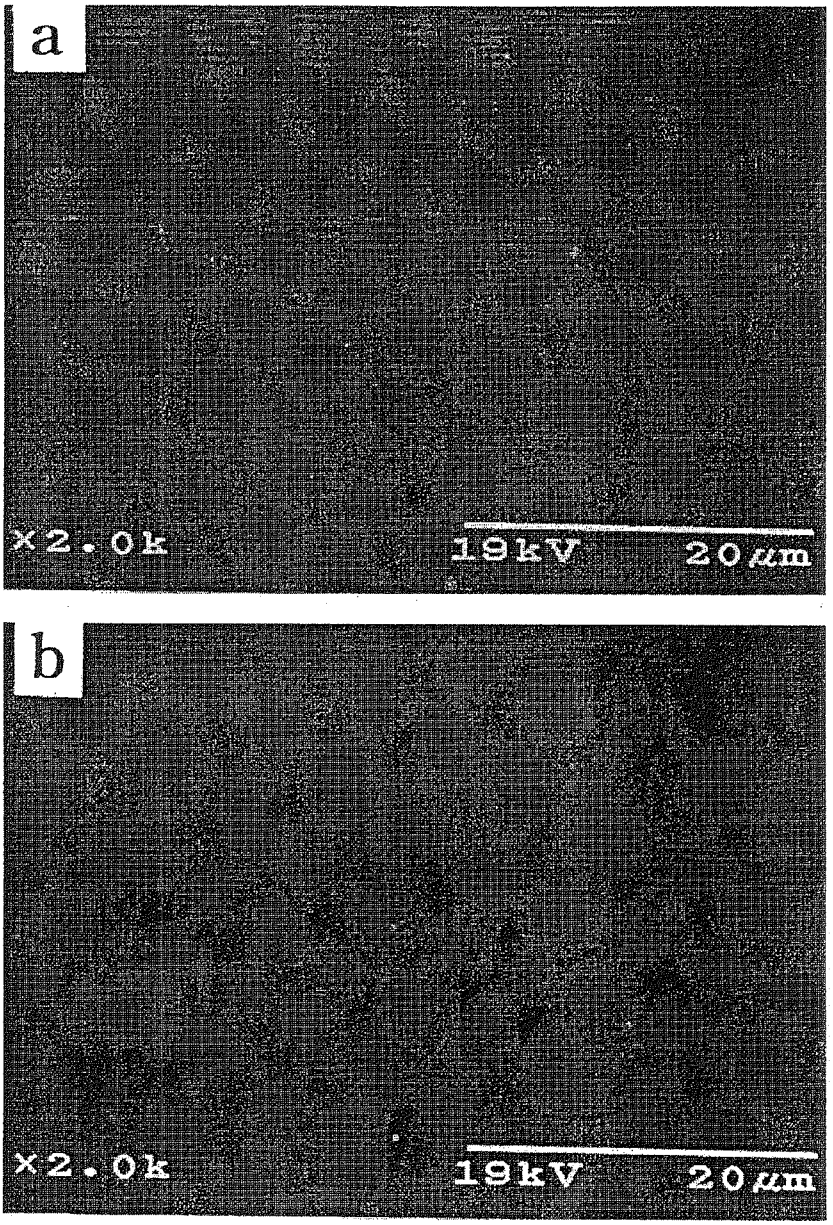

Figure 3. Typical SEM micrographs of (a) GL9 and (b) GL9-PEG8K-20 surfaces.

compared to the dried surfaces, the hydrophilic aspects of the wetted surfaces may have been exposed to the water phase by swelling in the hydrophilic environment.

The hydrophilicity of the network surfaces in the dried and wetted states was evaluated by measuring the static and dynamic contact angles at the air–water interface. Table 2 lists the contact angles obtained for the GL9-containing networks. The GL9 network showed relatively hydrophobic surfaces compared to GL9-PEG networks. The hydrophilicity increased both with increasing PEG molecular weight and content for the GL9-PEG networks, resulting from the introduction of hydrophilic PEG to the GL9 network surface, which was confirmed by ESCA analysis. In addition, after hydration in PBS for 1 day, the hydrophilicity was

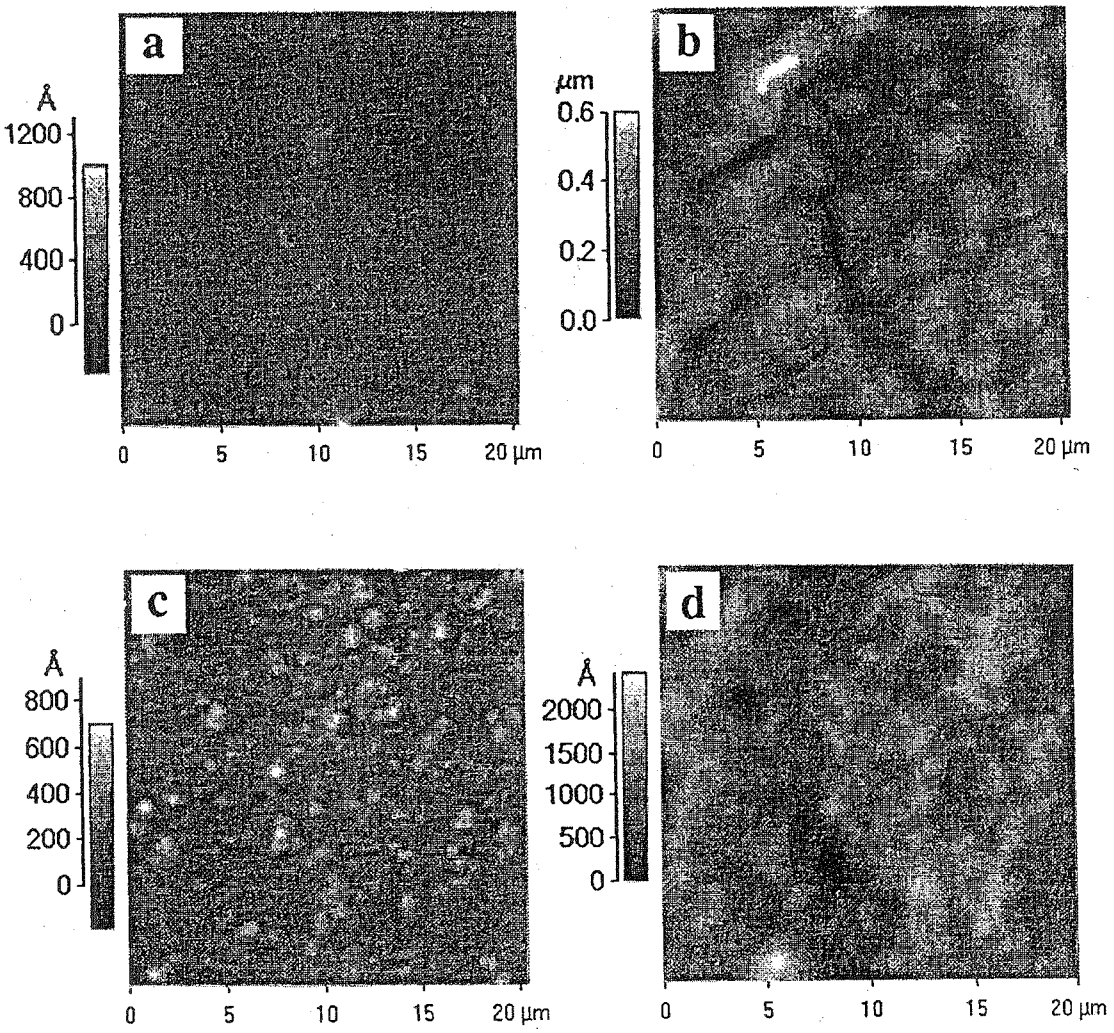

Figure 4. Typical AFM 2D images of GL9 and GL9-PEG surfaces: (a) GL9 network in dried state; (b) GL9-PEG8K-20 network in dried state; (c) GL9 network after hydration for 1 day; and (d) GL9-PEG8K-20 network after hydration for 1 day.

Table 2.
Contact angle results[a] for GL9 and GL9-PEG networks

Material	Static		Dynamic[b]	
	Dry	Wet[c]	θ_{adv}	θ_{rec}
GL9 network	70	65	92	58
GL9-PEG1K-20	50	43	85	55
GL9-PEG4K-10	46	39	78	50
GL9-PEG4K-20	43	35	73	45
GL9-PEG4K-30	40	31	69	42
GL9-PEG8K-20	37	26	67	40

[a] Unit: degree ($n = 3$–5).
[b] θ_{adv}: advancing contact angle; θ_{rec}: receding contact angle.
[c] After hydration in PBS for 24 h.

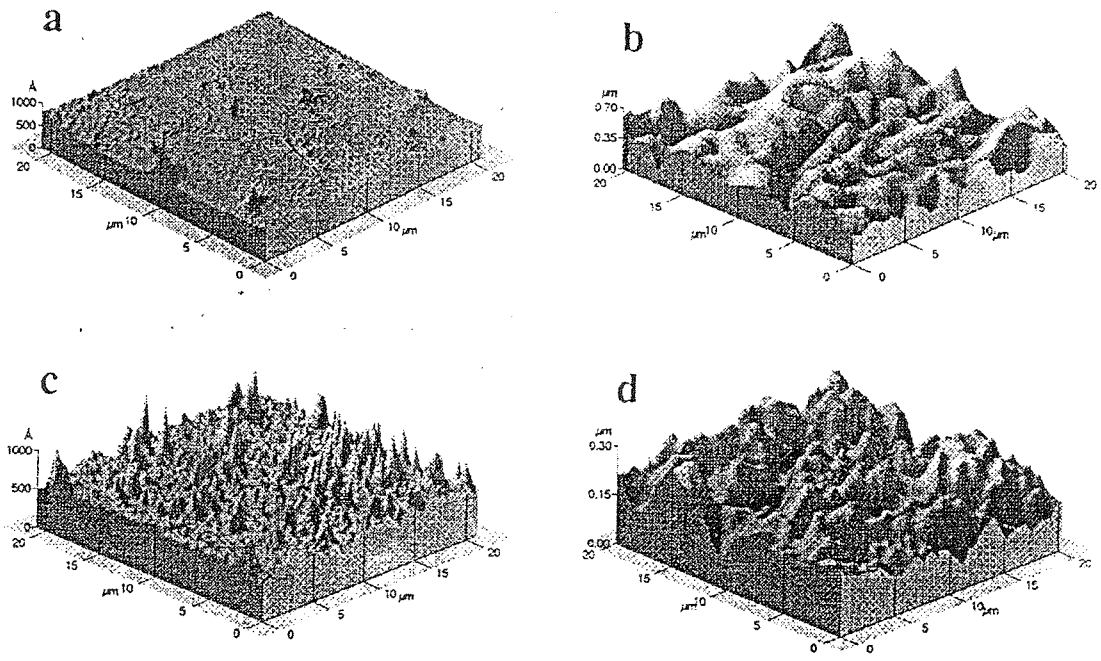

Figure 5. Typical AFM 3D images of GL9 and GL9-PEG surfaces: (a) GL9 network in dried state; (b) GL9-PEG8K-20 network in dried state; (c) GL9 network after hydration for 1 day; and (d) GL9-PEG8K-20 network after hydration for 1 day.

considerably increased in comparison with same samples before such extensive hydration. These results, specifically the observation at constant PEG content, suggest that the surfaces are more hydrophilic because the pendent PEG chains at the surfaces are highly mobile and are capable of rearrangement to minimize their interfacial free energy depending on the environment, such as air or water [25]. This interpretation of the contact angle measurement is consistent with the AFM observations. Accordingly, it seems that such surface properties of GL9-PEG networks might be expected to positively affect their biocompatibility.

Plasma protein adsorption

To quantify the adsorption on plasma proteins to GL9 and GL9-PEG network surfaces, the films were exposed to diluted plasma and the relative amounts of adsorbed proteins on the surfaces were evaluated by ESCA narrow scan spectra (Fig. 6). The nitrogen signal from peptide bonds in proteins was used as an indicator of surface protein adsorption, because all of the used samples have no nitrogen without adsorbed proteins. All GL9 and GL9-PEG surfaces showed lower protein adsorption than glass used as a reference material. The GL9 network lacking PEG exhibited a larger amount of protein adsorption than did the GL9-PEG networks, in which the flexible hydrophilic PEG chains were incorporated. As the PEG molecular weight and content were increased independently, the amount of adsorbed protein on GL9-PEG surfaces decreased. In particular, GL9-PEG8K-20 network showed the lowest protein adsorption of networks studied.

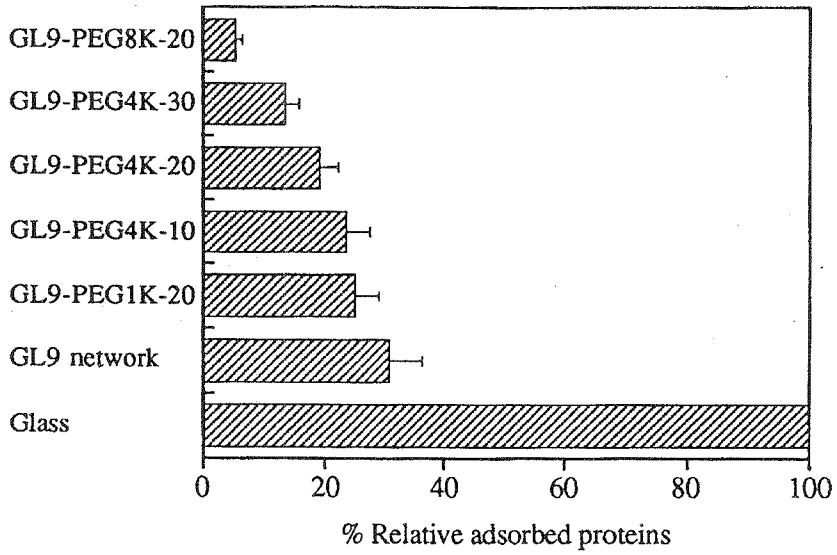

Figure 6. Relative amounts of protein adsorption on GL9 and GL9-PEG surfaces in plasma for 1 h ($n = 3-5$).

Many factors are involved in protein adsorption onto polymer surfaces. Of importance are hydrophobic interactions, electrostatic interactions, and acceptor–donor interactions [26]. It is well agreed that more protein generally adsorbs upon hydrophobic surfaces compared to hydrophilic surfaces, which is mainly attributed to hydrophobic interaction between protein and surface in which the protein acts as a surfactant. In the case of the GL9 network lacking PEG, the hydrophobic interaction of plasma proteins with hydrophobic lactide in the GL9 surface may induce relatively high levels of protein adsorption. It was reported that PEG-grafted polymer surfaces decreased significantly the extent of protein adsorption due to low interfacial free energy, highly dynamic motion and the extended chain conformation of PEG [8, 27, 28].

Platelet adhesion

PRP exposure was used to examine the adhesion behavior of platelets to the GL9 and GL9-PEG network surfaces (Fig. 7). GL9-PEG surfaces displayed relatively lower amounts of platelet adhesion and activation than did GL9 network lacking PEG. This trend was more remarkable when the PEG molecular weight was increased from 1000 to 8000 and its content was increased from 10 to 30%. The lowest amount of platelet adhesion was revealed on GL9-PEG8K-20 surface, that being reduced to 80% of the amount on the GL9 network lacking PEG.

It is highly likely that the reduced adhesion of platelets to GL9-PEG networks relative to GL9 is due to reduced levels of protein adsorption, as described above; adsorbed fibrinogen is known to be critically important in mediating platelet adhesion to materials, via interaction with GPIIb/IIIa receptor. This effect has been observed by others and is attributed to influence protein adsorption via the dynamic movement of the incorporated PEG [5, 9]. The greater the PEG molecular

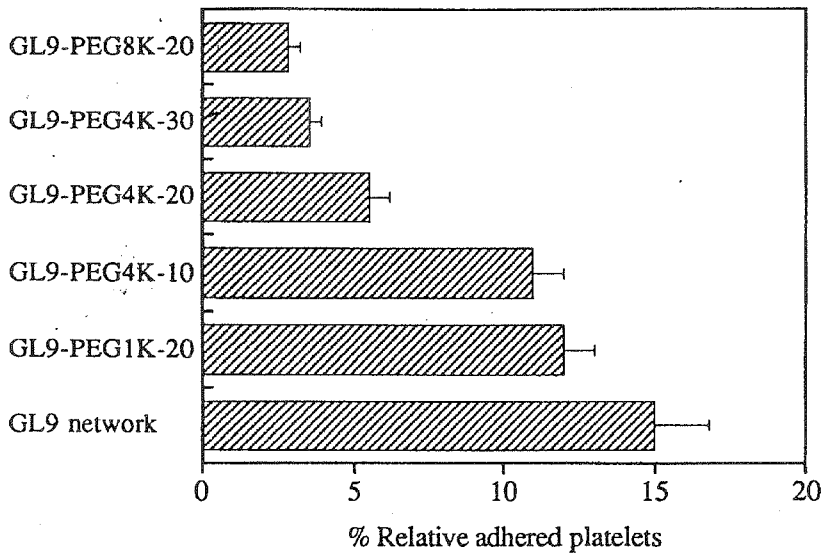

Figure 7. Relative platelet adhesion on GL9 and GL9-PEG surfaces in diluted PRP for 2 h ($n = 3-5$). 100% corresponds to adhesion of 6.7% of the platelets in the plasma sample.

weight is, the greater the expected molecular mobility would be, and thus the lower the adsorption of proteins and the adhesion of platelets. The results, therefore, suggest that longer PEG chain incorporated is more effective to minimize the platelet adhesion, perhaps resulting from both the volume restriction effect and local osmotic pressure effect of long chain molecules [27]. Such a suppressed platelet interaction of GL9-PEG networks may enhance blood compatibility in use as scaffolds in tissue/organ regeneration in the cardiovascular system.

Bacterial adhesion

Bacterial colonization of biomaterial surfaces and subsequent biomaterial-centered infection is known to be an important factor affecting biocompatibility. Bacterial adhesion to GL9 and GL9-PEG networks was evaluated using *S. epidermidis*, one of the bacteria that is commonly implicated in implant-related infections (Fig. 8).

As compared to the GL9 network surface, a significant decrease in bacterial adhesion was observed on GL9-PEG networks. Bacterial adherence on GL9-PEG surfaces was reduced notably with both increasing PEG molecular weight and content. In the case of the GL9 series, GL9-PEG8K-20 as well as GL9-PEG4K-30 showed similar low bacterial adhesion, which were reduced by approximately 90% relative to GL9 network lacking PEG.

The relationship between biomaterial properties and bacterial adhesion has been studied with the goal reducing infection in medical devices and implants. It has been reported that adsorbed plasma proteins such as fibrinogen and high molecular weight kininogen act as important mediators in the adherence of bacteria to biomaterial surfaces. Generally, bacteria adhere more on hydrophobic surfaces than on hydrophilic ones, an effect that is likely related to protein adsorption as described above [29, 30]. Relative to the hydrophobic GL9 surface, the hydrophilic

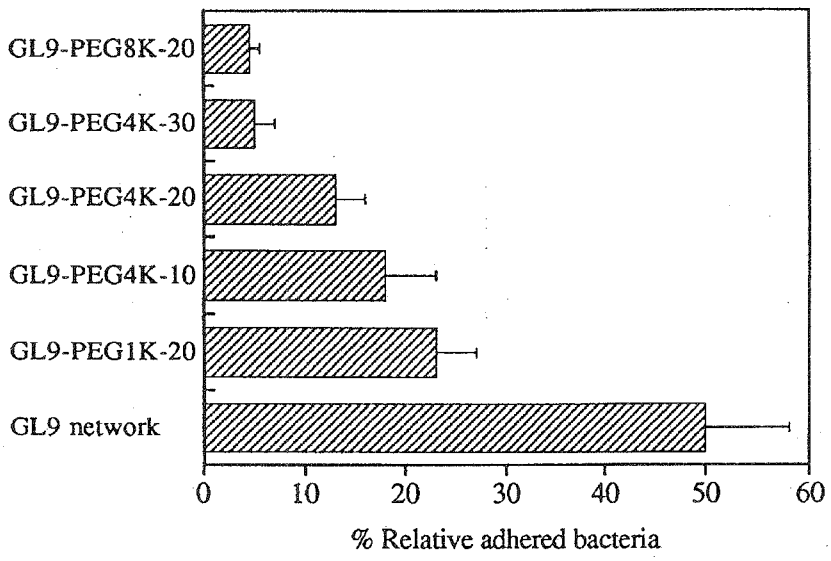

Figure 8. Relative *S. epidermidis* adhesion on GL9 and GL9-PEG surfaces ($n = 3-5$). 100% corresponds to 2.5×10^5 CFU.

GL9-PEG networks exhibited significantly decreased bacterial adhesion, which is consistent with other reports on polymer surfaces containing PEG [11, 31]. In addition, the effects of chain length and content of PEG were consistent with the results of protein adsorption and platelet adhesion presented above.

CONCLUSIONS

Two nontoxic macromers, triacrylated glycerol-lactide and monoacrylated PEG were copolymerized by UV photoinitiation to obtain new lactide-based PEG polymer network scaffolds. These surfaces were observed to be enriched with PEG, especially after the networks were hydrated, suggesting extensive reorganization in the aqueous environment. Such reorientation was correlated by imaging with SEM and AFM. Correlated behavior was consistently observed between an increase in surface hydrophilicity, a decrease in plasma protein adsorption, a decrease in platelet adhesion, and a decrease in *S. epidermidis* adhesion, all as either the PEG molecular weight was increased at constant mass content or as PEG mass content was increased at constant molecular weight. Given that these networks are constructed from nontoxic components and that the networks swell to a limited extent, and thus have good mechanical properties, they may be useful as scaffolds in tissue engineering.

Acknowledgement

This research was supported by Korea MOST grant V00194.

REFERENCES

1. R. Langer and J. P. Vacanti, *Science* **260**, 920 (1993).
2. R. M. Nerem and A. Sambanis, *Tissue Eng.* **1**, 3 (1995).
3. J. A. Hubbell and R. Langer, *Chem. Eng. News* March 13, 42 (1995).
4. J. A. Hubbell, *Bio/Technology* **13**, 565 (1995).
5. J. D. Andrade, S. Nagaoka, S. L. Cooper, T. Okano and S. W. Kim, *Am. Soc. Artif. Intern. Organs J.* **10**, 75 (1987).
6. Y. H. Kim, K. D. Park and D. K. Han, in: *Polymeric Materials Encyclopedia*, J. C. Salamone (Ed.), Vol. 1, p. 825. CRC Press, Boca Raton, FL (1996).
7. M. Amiji and K. Park, *J. Biomater. Sci. Polymer Edn* **4**, 217 (1993).
8. D. K. Han, K. D. Park, G. H. Ryu, U. Y. Kim, B. G. Min and Y. H. Kim, *J. Biomed. Mater. Res.* **30**, 23 (1996).
9. D. K. Han, S. Y. Jeong, Y. H. Kim, B. G. Min and H. I. Cho, *J. Biomed. Mater. Res.* **25**, 561 (1991).
10. A. S. Sawhney, C. P. Pathak and J. A. Hubbell, *Macromolecules* **26**, 581 (1993).
11. N. P. Desai, S. F. A. Hossainy and J. A. Hubbell, *Biomaterials* **13**, 417 (1992).
12. F. Fuerteges and A. Abuchowski, *J. Control. Rel.* **11**, 139 (1990).
13. J. H. Lee, P. Kopeckova, J. Kopecek and J. D. Andrade, *Biomaterials* **11**, 455 (1990).
14. J.-H. Chen and E. R. Stein, *J. Colloid Interface Sci.* **142**, 545 (1991).
15. D. K. Han, S. Y. Jeong and Y. H. Kim, *J. Biomed. Mater. Res.: Appl. Biomater.* **23** (A2), 211 (1989).
16. K. D. Park, W. G. Kim, H. Hacobs, T. Okano and S. W. Kim, *J. Biomed. Mater. Res.* **26**, 739 (1992).
17. Y. C. Tseng and K. Park, *J. Biomed. Mater. Res.* **26**, 373 (1992).
18. M. S. Sheu, A. S. Hoffman, J. G. A. Terlingen and J. Feijen, *Clin. Mater.* **13**, 41 (1993).
19. D. K. Han and J. A. Hubbell, *Macromolecules* **29**, 5233 (1996).
20. D. K. Han and J. A. Hubbell, *Macromolecules* **30**, 6077 (1997).
21. J. D. Andrade, in: *Surface and Interfacial Aspects of Biomedical Polymers*, J. D. Andrade (Ed.), Vol. 1, Chap. 5. Plenum Press, New York (1985).
22. D. K. Han, S. Y. Jeong, Y. H. Kim and B. G. Min, *J. Appl. Polym. Sci.* **47**, 761 (1993).
23. L. Smith, C. Doyle, D. E. Gregonis and J. D. Andrade, *J. Appl. Polym. Sci.* **27**, 1269 (1982).
24. J. H. Lee, B. J. Jeong and H. B. Lee, *J. Biomed. Mater. Res.* **34**, 105 (1997).
25. D. K. Han, S. Y. Jeong, K.-D. Ahn, Y. H. Kim and B. G. Min, *J. Biomater. Sci. Polymer Edn* **4**, 579 (1993).
26. J. D. Andrade and V. Hlady, *Ann. NY Acad. Sci.* **516**, 158 (1987).
27. Y. Mori, S. Nagaoka, H. Takiuchi, N. Kikuchi, N. Noguchi, H. Tanzawa and Y. Noishiki, *Trans. Am. Soc. Artif. Intern. Organs* **28**, 459 (1982).
28. E. W. Merrill and E. W. Salzman, *Am. Soc. Artif. Intern. Organs J.* **6**, 60 (1983).
29. J. Dankert, A. H. Hogt and J. Feijen, *CRC Crit. Rev. Biocompat.* **2**, 219 (1986).
30. S. Nagaoka and H. Kawakami, *Am. Soc. Artif. Intern. Organs J.* **41**, 365 (1995).
31. K. D. Park, Y. S. Kim, D. K. Han, Y. H. Kim, E. H. B. Lee, H. Suh and K. S. Choi, *Biomaterials* (1998) (in press).